Journal of Alloys and Compounds, 190 (1993) 243–247
JALCOM 439

Study of the electrical conduction behaviour of the $Ba_{1-x}La_xTi_{1-x}Ni_xO_3$ ($x \leqslant 0.10$) system

Om Parkash
School of Materials Science and Technology, Institute of Technology, Banaras Hindu University, Varanasi 221005 (India)

H. S. Tewari and V. B. Tare
Department of Metallurgical Engineering, Institute of Technology, Banaras Hindu University, Varanasi 221005 (India)

D. Kumar
Department of Ceramic Engineering, Institute of Technology, Banaras Hindu University, Varanasi 221005 (India)

(Received May 12, 1992; in final form July 25, 1992)

Abstract

The electrical conduction behaviour of the $Ba_{1-x}La_xTi_{1-x}Ni_xO_3$ ($x \leqslant 0.10$) system has been studied by complex plane impedance analysis and measurements of a.c. conductivity in the temperature range 400–575 K. The values of the bulk resistance for these samples are obtained from a circular arc passing through the origin in their impedance plots. A.c. conductivity obeys the relation $\sigma_{a.c.} \propto \omega^s$ in the temperature range of measurements. These results indicate that conduction occurs in this system because of hopping of charge carriers between localized nickel sites.

1. Introduction

We have been investigating the possibility of formation of valence-compensated solid solutions of the type $M_{1-x}La_xTi_{1-x}Co_xO_3$ (M ≡ Pb, Ba, Sr and Ca) [1–4] for the last few years and studying their electrical behaviour [5–8]. Some compositions exhibit dielectric relaxor behaviour in the systems exhibiting high values of the dielectric constant [9–11]. These materials may find application in multilayer ceramic capacitors. The cobalt ions in these systems are found to play an important role in the electrical conduction behaviour. In view of the interesting and useful properties of these systems, it was considered worthwhile to explore the properties and potential use of analogous systems in which cobalt is replaced by nickel. Recently, the possibility of formation of the solid solution $Ba_{1-x}La_xTi_{1-x}Ni_xO_3$ for $x \leqslant 0.50$ was investigated [12]. This represents a solid solution between $BaTiO_3$ (an insulator) and $LaNiO_3$ (a Pauli paramagnetic metal) [13]. It was found that the compositions with $x \leqslant 0.10$ form a single-phase solid solution while the compositions with $x \geqslant 0.15$ were found to be multiphase materials as indicated by their X-ray powder diffraction data. Only the composition with $x = 0.01$ has been found to exhibit dielectric anomaly at about 353 K characteristic of the ferroelectric-to-paraelectric transition. The microstructure of this composition also shows the domain structure, while the compositions with $x = 0.05$ and $x = 0.10$ do not show the domain structure [12].

In this paper we report the electrical conduction behaviour of the compositions with $x = 0.01$, 0.05 and 0.10. Measurement of d.c. resistance in these high resistivity samples is difficult because of effects associated with electrode polarization. Hence we have employed complex plane impedance analysis to study the electrical conduction behaviour of these materials. The charge transport through the solids have the following three contributions; (i) the contribution from grains known as intergranular or bulk conduction designated by G_b; (ii) the contribution from the grain boundaries designated as G_{gb}; (iii) the contribution from the solid–electrode interfaces known as G_{el}. The corresponding resistances are represented by R_b, R_{gb} and R_{el}. Each of these contributions can be represented by a suitable combination of resistance and capacitance in parallel. The sample can thus be represented by an equivalent circuit containing three parallel R–C circuits connected in series. The total complex impedance Z^* of the sample is given by

$$Z^* = Z' - iZ''$$

where Z' and Z'' are the real and imaginary parts of the impedance. In complex plane impedance analysis,

0925-8388/93/$6.00

the imaginary part Z'' of the impedance is plotted as a function of the real part Z' over a range of frequencies. Three semicircular arcs are usually obtained. The arc with the lowest frequency range generally corresponds to electrode polarization, the arc with intermediate frequency range represents the grain boundary contribution to the observed resistance and the arc with the highest frequency range passing through the origin represents the grain or bulk resistance. These resistances are obtained from the intercept of these arcs with the Z' axis. If each of the above processes has a single value of relaxation time, then the circular arcs have their centres on the Z' axis. If there is a distribution of relaxation times for any of these processes, then one obtains a depressed circular arc in the complex impedance plot having its centre below the Z' axis. The details of complex plane impedance analysis for various possibilities of the three circuit elements mentioned above are available in the literature [14–17].

Complex plane impedance analysis has been used extensively to delineate the various contributions to the total observed resistance in the solid electrolytes exhibiting predominantly ionic conduction [18]. It has also been found to be equally useful for semiconducting barium titanate showing the positive temperature coefficient of resistance effect [19]. In the present work we have used this technique to investigate the resistivity behaviour of our samples.

2. Experimental details

Compositions with $x=0.01$, 0.05 and 0.10 were prepared by the ceramic method using barium carbonate, lanthanum oxalate, titanium dioxide and basic nickel carbonate, all having purities better than 99.5%. Appropriate quantities of these materials were weighed accurately and mixed in an agate mortar using acetone. The dried powders were calcined at 1523 K in a platinum crucible for 12 h and then furnace cooled. The resulting powders were ground and mixed with 1% solution of polyvinyl alcohol and pressed as cylindrical pellets. These pellets were slowly heated to 873 K and kept at this temperature for 1 h to burn off the binder. The temperature was then raised to 1573 K; the pellets were sintered at this temperature for 24 h and then cooled in the furnace in air.

X-ray powder diffraction patterns of the final products were taken in a X-ray diffractometer (JEOL) using Cu Kα radiation. For conductivity measurements, flat polished surfaces of pellets were coated with air-dried silver paint after washing with isopropyl alcohol and heating at 423 K to remove any adsorbed moisture. The conductance G was measured as a function of frequency at different steady temperatures in the temperature range 400–575 K with an impedance analyser (Hewlett–Packard 4192A LF). Measurements were limited to 575 K because the silver paint used as electrodes cannot be used above this temperature.

3. Results and discussion

From the measured values of conductance G and dissipation factor D, Z' and Z'' were calculated by the following relations:

$$Z' = \frac{G}{G^2+\omega^2C^2} \tag{1}$$

$$Z'' = \frac{\omega C}{G^2+\omega^2C^2} \tag{2}$$

where $\omega = 2\pi f$, ω is the angular frequency and f is the frequency in cycles per second. Z'' has been plotted as a function of Z' for the frequency range 100 Hz–1 MHz. Typical impedance plots for these samples are shown in Figs. 1–3 at a few temperatures. The data in these figures have been fitted manually. This may involve some uncertainty in the resistance values obtained. Since finally we are plotting the logarithm of resistivity to find the activation energy of conduction, the error involved will be negligible. At low temperatures, only one circular arc appearing to pass through the origin is obtained. At higher temperatures, another arc starts to appear in the low frequency range. This appearance of the low frequency arc at high temperatures may be due to either the grain boundary contribution or the electrode–specimen interface contribution. More experiments are required to ascertain

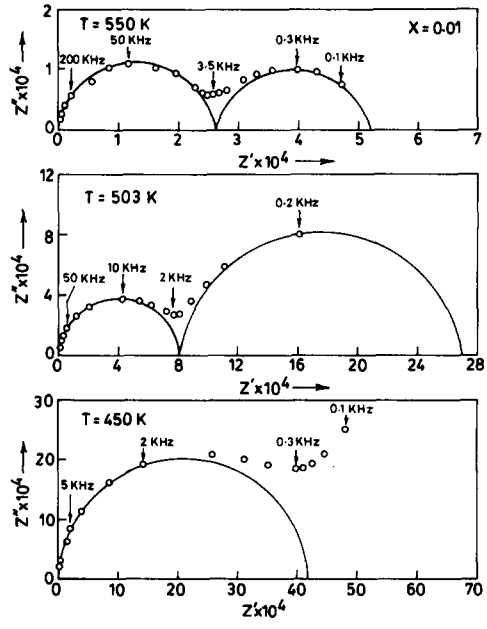

Fig. 1. Impedance plots of $Ba_{0.99}La_{0.01}Ti_{0.99}Ni_{0.01}O_3$.

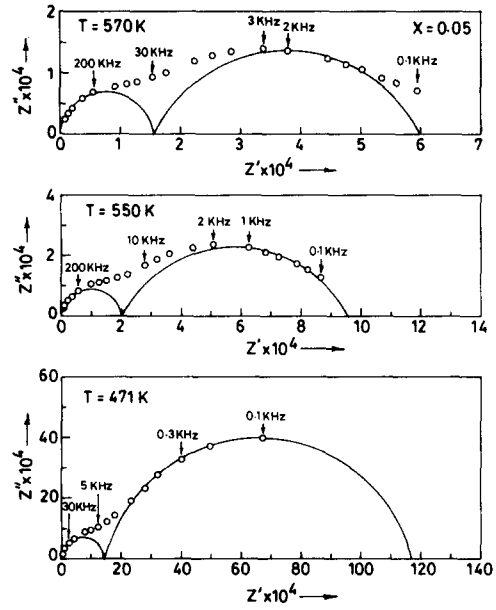

Fig. 2. Impedance plots of the $Ba_{0.95}La_{0.05}Ti_{0.95}Ni_{0.05}O_3$ system.

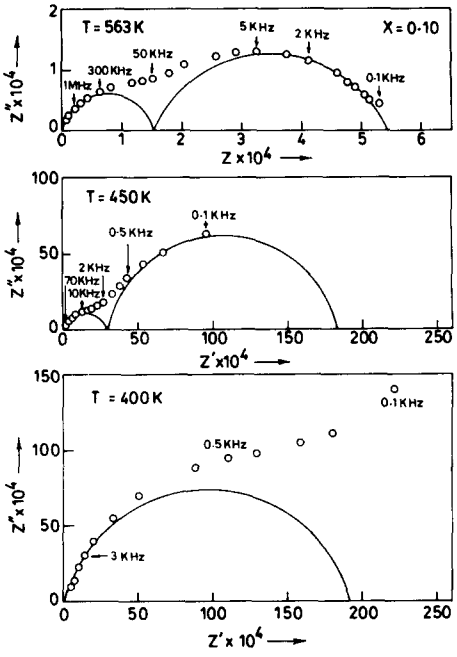

Fig. 3. Impedance plots of $Ba_{0.90}La_{0.10}Ti_{0.90}Ni_{0.10}O_3$.

this. For the present we shall consider only the arc passing through the origin which represents the bulk conduction. Values of the bulk resistance were found by the intersection of this circular arc with Z' axis from which the corresponding resistivities were calculated. Plots of the logarithm $\log \rho_b$ of the bulk resistivity as a function of the inverse temperature $1000/T$ are shown in Fig. 4. These plots are linear, showing that resistivity obeys an Arrhenius relationship

$$\rho = \rho_0 \exp\left(\frac{E_a}{kT}\right) \tag{3}$$

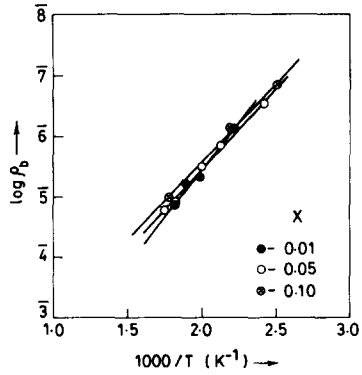

Fig. 4. Plots of $\log \rho_b$ *vs.* $1000/T$ for the $Ba_{1-x}La_xTi_{1-x}Ni_xO_3$ system.

TABLE 1. Activation energy E_a for d.c. conductivity, E_a' activation energy for a.c. conductivity at 100 kHz and hopping energy W for various samples in the $Ba_{1-x}La_xTi_{1-x}Ni_xO_3$ system

x	E_a (eV)	E_a' (eV)	W (eV)
0.01	0.62	0.59	0.03
0.05	0.52	0.38	0.14
0.10	0.51	0.33	0.18

where E_a is the activation energy for conduction. The values of E_a obtained by least-squares fitting of the data in these plots (Fig. 4) are given in Table 1.

Barium titanate is a wide band gap material similar to TiO_2 in which the filled valence band consisting of O 2p orbitals is separated from the empty conduction band of Ti 4s orbitals by 3.0 eV [20]. The values of activation energies obtained (Table 1) rule out the possibility of any intrinsic conduction in these materials. It has been reported that Ni^{2+} gives rise to energy levels at about 0.8 eV above the 2p band of oxygen ions in TiO_2 [20]. This will also be true for $BaTiO_3$. The conduction therefore seems to occur through localized Ni^{2+} and Ni^{3+} sites in the present system. The generation of Ni^{2+} in these materials can be understood as follows. These materials are expected to lose traces of oxygen during their sintering at high temperatures in accordance with the reaction

$$O_O \longrightarrow \tfrac{1}{2}O_2 + V_O^{\cdot\cdot} + 2e' \tag{4}$$

where all the species are written in accordance with the Kröger-Vink notation for defects [21]. Two electrons released in the process may be captured by Ni^{3+} or Ti^{4+} to produce Ni^{2+} or Ti^{3+} ions respectively. Since Ti^{4+} has the closed-shell configuration of argon gas, generation of Ti^{3+} seems to be highly unlikely in air. Thus these materials will contain a small amount of divalent nickel Ni^{2+} ions. Electrical conduction in these

materials may therefore occur through hopping of charge carriers between localized Ni^{2+} and Ni^{3+} sites.

In order to understand the mechanism of conduction, we have plotted log $\sigma_{a.c.}$ as a function of log f (where f is frequency) at two temperatures in Fig. 5. We have plotted the a.c. conductivity data above 10 kHz to consider only the bulk effect. It is found that $\sigma_{a.c.}$ varies as

$$\sigma_{a.c.} = Aw^s \tag{5}$$

where $w = 2\pi f$ is the angular frequency. The values of s obtained by least-squares fitting of the data are in the range 0.6–0.7 at 300 K. The value of s decreases with increasing temperature. The frequency dependence of $\sigma_{a.c.}$ may arise as a result of (i) hopping of charge carriers between localized sites, giving rise to debye-type loss similar to thermally activated rotation of dipoles [22] (this will give rise to a.c. conductivity proportional to T if compensation is large [23] and independent of T if the compensation is small [22]), (ii) hopping of charge carriers between localized sites at energies close to E_F and (iii) excitation of charge carriers at the band edge and hopping at energies close to it. This latter process gives rise to an a.c. conductivity whose variation with temperature is similar to that of carrier concentration *i.e.* $\sigma_{a.c.} \alpha \exp[-(E_F - E_A)/kT]$, where E_A is the valence band edge. The variation in d.c. conductivity in this mechanism is given by $\sigma_{d.c.} \alpha \exp\{-[(E_F - E_A + W)/kT]$, where W is the activation energy for hopping of charge carriers.

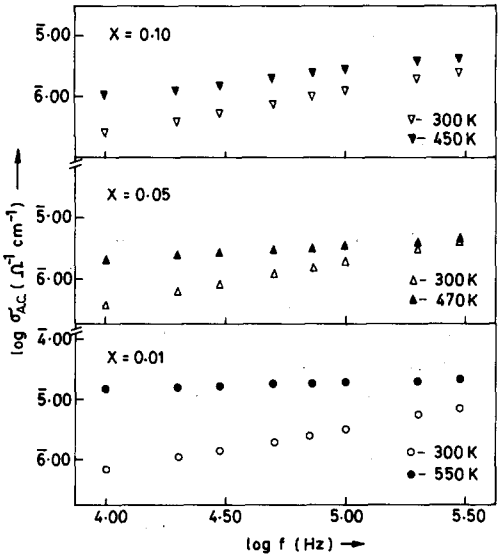

Fig. 5. Variation in log $\sigma_{a.c.}$ as a function of frequency for the $Ba_{1-x}La_xTi_{1-x}Ni_xO_3$ system.

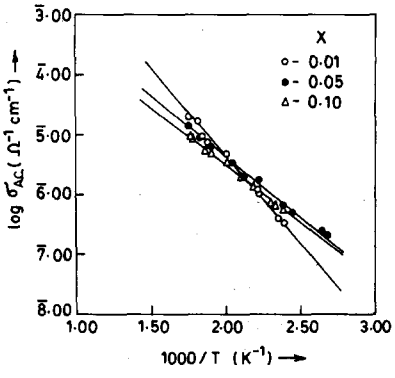

Fig. 6. Plots of log $\sigma_{a.c.}$ *vs.* $1000/T$ at 100 kHz for the $Ba_{1-x}La_xTi_{1-x}Ni_xO_3$ system.

Plots of log $\sigma_{a.c.}$ *vs.* $1000/T$ for all the samples at 100 kHz are shown in Fig. 6. We have plotted the data at 100 kHz so that it represents only the bulk behaviour. The observed exponential dependence of a.c. conductivity on temperature (Fig. 6) shows that the conduction occurs by mechanism (iii). The difference between the activation energies of conduction for d.c. and a.c. conductivity gives the activation energy for hopping. These values are given in Table 1. It is found that W increases with increasing x. This may be due to increasing disorder with increase in x. A similar conduction mechanism operates in the analogous systems $Ba_{1-x}La_xTi_{1-x}Co_xO_3$ and $Ca_{1-x}La_xTi_{1-x}Co_xO_3$ where direct measurement of d.c. conductivities were made above 400 K [6, 8]. This shows the effectiveness of the complex plane impedance analysis in studying the conduction behaviour in these complex high resistivity materials at low temperatures.

Acknowledgment

We are grateful to Department of Science and Technology, Government of India, New Delhi, for financial support.

References

1 O. Parkash, C. D. Prasad and D. Kumar, *J. Solid State Chem., 69* (1987) 385.
2 O. Parkash, C. D. Prasad and D. Kumar, *J. Mater. Sci. Lett., 8* (1989) 475.
3 O. Parkash, C. D. Prasad and D. Kumar, *Phys. Status Solidi A, 116* (1989) K81.
4 O. Parkash, C. D. Prasad and D. Kumar, *Bull. Mater. Sci., 11* (1988) 39.
5 D. Kumar, C. D. Prasad and O. Parkash, *Bull. Mater. Sci., 9* (1987) 123.
6 D. Kumar, C. D. Prasad and O. Parkash, *J. Phys. Chem. Solids, 51* (1990) 73.
7 O. Parkash, C. D. Prasad and D. Kumar, *J. Phys. Chem. Solids,* submitted for publication.
8 O. Parkash, D. Kumar, C. D. Prasad and H. S. Tewari, *J. Phys. D, 23* (1990) 423.
9 O. Parkash, C. D. Prasad and D. Kumar, *Phys. Status Solidi A, 106* (1988) 627.
10 O. Parkash, C. D. Prasad and D. Kumar, *J. Mater. Sci., 25* (1990) 487.

11 C. D. Prasad, H. S. Tewari, D. Kumar and O. Parkash, *Bull. Mater. Sci., 11* (1988) 307.
12 O. Parkash, H. S. Tewari, L. Pandey, R. Kumar and D. Kumar, *J. Am. Ceram. Soc., 72* (1989) 1520.
13 P. Ganguly and C. H. R. Rao, *Mater. Res. Bull., 8* (1973) 405.
14 J. E. Bauerle, *J. Phys. Chem. Solids, 30* (1969) 2657.
15 J. R. Macdonald, *J. Chem. Phys., 61* (1974) 3977.
16 A. D. Franklyn, *J. Am. Ceram. Soc., 58* (1975) 465.
17 I. M. Hodge, M. D. Ingram and A. R. West, *J. Electroanal. Chem., 74* (1976) 125.
18 A. Hooper, *J. Phys. D, 10* (1977) 1487.
19 H. S. Maiti, *Mater. Res. Bull., 21* (1986) 1107.
20 K. Mizushima, M. Tanaka and S. Iida, *J. Phys. Soc. Japan, 32* (1972) 1519.
21 I. Burn and S. Neirman, *J. Mater. Sci., 17* (1982) 3510.
22 N. F. Mott and E. A. Davis, *Electronic Processes in Non-crystalline Materials*, Clarendon, Oxford, Chapter 6.
23 M. Pollak and T. N. Geballe, *Phys. Rev., 122* (1961) 1742.